# International Journal of Engineering Research and Science & Technology

IJERST

ISSN : 2319-5991

www.ijerst.com

Email: editor@ijerst.com or editor.ijerst@gmail.com

International Journal of Engineering Research and Science & Technology

ISSN 2319-5991 www.ijerst.com

Vol. 11, Issue 4, 2018

# INNOVATIVE EXTREME FAST CHARGING STATIONS FOR ELECTRIC VEHICLES WITH ENHANCED PARTIAL POWER PROCESSING

[1]Easlavath Hathiram,[2]Babu Rao Paddam,[3]Akula Jeevan
[1]Assistant Professor,[2]HOD& Assoc.Prof,[3]Student

*Department of EEE*

*Abdul Kalam Institute of Technological Sciences, Kothagudem, Telangana*

**ABSTRACT:** The power supply plan for an extreme fast charging (XFC) station, which is intended to charge many electric cars (EVs) at once, is proposed in this article. Galvanic isolation is achieved by means of dual-active-bridge based soft-switched solid-state transformers, while a cascaded H-bridge converter is used for direct medium voltage grid interface. By charging each EV separately using partial power rated dc–dc converters, the suggested method does away with redundant power conversion. While only processing a portion of the overall battery charging power, partial power processing allows for individual charging control over each electric vehicle. Analysis is done on workable implementation plans for the partial power charger unit. A charger based on a phase-shifted full-bridge converter is suggested. Clear explanations of the design and control factors are provided for permitting numerous charging stations. The control characteristics, functionality, and efficacy of the proposed XFC station power supply method are validated by the presentation of experimental findings obtained from a downscaled laboratory test-bed. An efficiency increase of 0.6% at full load and 1.6% at 50% load is proven using a downscaled partial power converter designed to handle just 27% of the battery power.

**Keywords:** dual active bridge (DAB), fast charging station, Cascaded H-bridge (CHB) converter, dc fast charger, dc–dc power converters, energy storage

## I.INTRODUCTION

Transport sector accounts for about 23% of the global energy-related CO2 emissions with an annual emissions growth rate of 2.5% between 2010 and 2015. Transportation electrification is expected to play a major role in decarbonizing transport sector. Superior performance, lower operating cost, reduced greenhouse gas emissions, improvement in the battery technology and driving range, along with the reduction in the vehicle cost have led to significant increase in the adoption rate of Battery Electric Vehicles (BEVs) and Plug-in Hybrid Electric Vehicles (PHEVs) [1]. Analysis indicates that the lack of EV charging infrastructure and prolonged charging time can lead to driving range anxiety [2]. AC level 1 charging (< 2 kW) or AC level 2 charging (> 2 kW and < 10 kW) is most frequently used in a residential or workplace setting. AC level 2 charging is also typically used at both private and public facilities. For longer commutes, DC fast charging (> 20 kW and < 120 kW) stations are being deployed [3]. However, the charging time of BEV with a DC fast charger is still significantly higher than the refill time of the equivalent internal combustion engine vehicle. Therefore, it is envisaged that an Extreme Fast Charging (XFC) system (> 300 kW) is required to alleviate range anxiety and enable the widespread adoption of long range EVs [4], [5]. XFC system for a 300-mile range vehicle can cost up to $100,000 per system. In addition, it requires special equipment, installation procedures, permits and costly maintenance warranties [6].

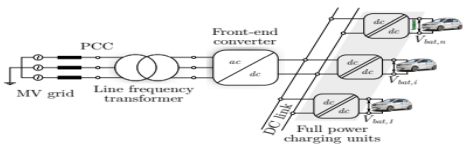


(a)

International Journal of Engineering Research and Science & Technology

ISSN 2319-5991 www.ijerst.com

Vol. 11, Issue 4, 2018

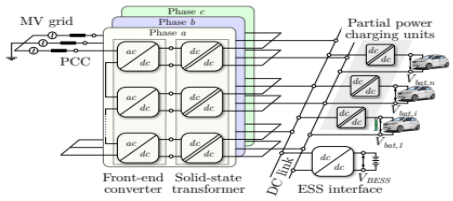


(b)

Fig. 1: XFC station architecture. (a) Conventional scheme with full rated charging converters. (b) Proposed scheme with partial rated charging converters.

Therefore, such a system will be typically owned by commercial customers or EV manufacturers. Several XFC systems can be arranged together to form an XFC station. Since an XFC station constitutes multiple XFC systems, it presents an opportunity for the reduction of capital investment and operating costs to make it economically viable. The common approach of realizing an XFC station is to have a centralized front-end converter (FEC) unit that interfaces with the Medium Voltage (MV) grid using a line frequency transformer as shown in Fig. 1a [7]–[10]. The weight, size, volume and large footprint of the line frequency transformer are serious concerns, especially in urban areas where cost of land is high. A direct MV grid interfaced fast charging station that utilizes a modular multilevel cascaded H-bridge (CHB) based front-end converter is reported in [5]. Dedicated full-rated DC-DC converter units are used for realizing the battery charging stage of the XFC system in all these approaches. In this work, a novel power delivery architecture for an XFC station based on partial power charging units (PPCUs) is proposed and is depicted in Fig. 1b. The CHB based frontend and the SST units are retained from [5]. Unlike in [5], the proposed solution offers a common low-voltage (LV) DC link which can interface with local DC microgrids such as a building based microgrid. In order to reduce stress on the grid infrastructure and to avoid excess demand charges, centralized energy storage and on-site energy generation can be integrated to the common DC link.

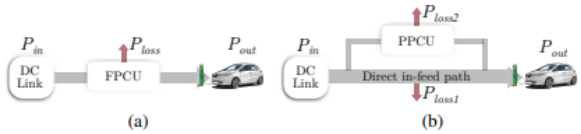


Fig. 2: Representative power flow diagram. (a) Full power charging unit. (b) Series-pass partial power charging unit.

The power rating of the CHB and SST units can be significantly reduced with such local energy storage solutions. The novelty of the proposed scheme lies in the use of DCDC converters that employ partial power processing for each charging point as against the full power DC-DC converter based charging solution reported in literature. The charging units are rated only to handle a fraction of the power required for battery charging. This approach can potentially reduce the installation and operational costs in an XFC station and simultaneously improve the overall system efficiency. In literature, partial power processing is also referred to as differential power processing [11]. A partial power converter is configured as a series element or a parallel element with the load that processes only a fraction of the total power [12]. The terminal connection configuration of a traditional power converter is typically modified to emulate it as a partial power processing element. Partial power processing converters have been successfully used to enhance system performance in a variety of applications such as photovoltaic panel integration [12]–[14], thermoelectric generation systems [15], [16], datacenter power delivery schemes [17], EV battery charging systems [18], [19], etc. Partial power processing based XFC station concept has been proposed in the conference version of this work [18]. In this paper, the concept has been expanded and treated in a systematic manner with extensive system level analysis and cell level experimental validation. The specific contributions of this paper are listed below:
1) Unidirectional, series-type partial power conversion schemes suited for extreme fast battery charging application are elucidated, and their performance compared. System level benefits of using a partial power conversion scheme are analyzed .

2) A practical, partial power charging unit is conceptualized and its design considerations are discussed [Section. III].

3) Modeling and control considerations of the partial power charging unit are discussed and a control strategy suited for battery charging is proposed.

International Journal of Engineering Research and Science & Technology

ISSN 2319-5991 www.ijerst.com

Vol. 11, Issue 4, 2018

4) Experimental results obtained from a hardware prototype developed in the laboratory are presented to showcase the functionality, control aspects and effectiveness of the proposed approach.

## II. PARTIAL POWER CHARGING UNIT (PPCU)

As opposed to a conventional charging unit that processes the full power delivered to the EV battery as shown in Fig. 2(a), the PPCU processes only a fraction of that power, as shown in Fig. 2(b). Bulk power is transferred to the EV battery through a direct infeed path. The PPCU enables battery charging at a controlled rate and can be envisaged as an active series-pass element that is used to interface the EV to the XFC station dc link. The desired operational features of the PPCU are listed as follows.

The PPCU should facilitate power transfer from the dc link to the EV battery at a controlled rate without consuming any power.

The PPCU should not introduce any circulating current between two or more charging points.

The PPCU should meet ripple voltage and current specifications as recommended by IEC 61851-23:2014 [20].

Such a PPCU can be practically realized using a traditional two-port dc–dc power converter. Any one port of the PPCU gets connected in series with the EV battery such that the voltage difference between the dc link and the EV battery is impressed upon it. The power processed by the converter is regenerated by connecting the other port of the PPCU to either the dc link or the EV battery. An isolated dc–dc converter topology is typically employed to facilitate regeneration. Past literature discusses several partial power converter realizations. However, a generic treatment, in terms of the various connection schemes to realize the partial power converter, is missing.

Universal schemes for realizing a series-pass PPCU are listed in Table I. Without loss of generality, it is assumed that power flows from Port 1 to Port 2 in the PPCU. All of these schemes.

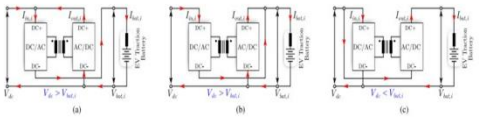

Fig. 3. Feasible partial power charger unit implementation schemes based on unidirectional isolated dc–dc converters that utilizes unidirectional voltage blocking switches. (a) Scheme 1 (Vdc > Vbat,i). (b) Scheme 2 (Vdc > Vbat,i). (c) Scheme 3 (Vdc < Vbat,i).

TABLE I

UNIVERSAL SCHEMES FOR PPCU REALIZATION

| DC Voltage - Port 1 $V_{in,i}$ | DC Voltage - Port 2 $V_{out,i}$ | Feasibility for battery charging |
|---|---|---|
| $V_{dc} - V_{bat,i}$ | $V_{dc}$ | Yes |
| $V_{bat,i} - V_{dc}$ | $V_{dc}$ | No |
| $V_{dc} - V_{bat,i}$ | $V_{bat,i}$ | Yes |
| $V_{bat,i} - V_{dc}$ | $V_{bat,i}$ | No |
| $V_{dc}$ | $V_{dc} - V_{bat,i}$ | No |
| $V_{dc}$ | $V_{bat,i} - V_{dc}$ | Yes |
| $V_{bat,i}$ | $V_{dc} - V_{bat,i}$ | No |
| $V_{bat,i}$ | $V_{bat,i} - V_{dc}$ | No |

May not be suitable for a battery charging application and need to be further examined. The following constraints are imposed to down select the configurations suited for battery charging.

Reverse power flow from EV battery (vehicle-to-grid or V2G operation) is not considered.

Unidirectional voltage blocking switches are used for realizing the PPCU.

Since the proposed versatile XFC station has a central BESS unit that can be used to support advanced features, such as grid frequency regulation and peak shaving, there may not be much merit in incorporating V2G feature. Additionally, the XFC station will be typically owned by commercial customers and V2G may not be required. Hence, unidirectional charging converters are considered in this article. An additional physical constraint is imposed by the semiconductor choice for the PPCU. The dc voltage seen at any port has to be positive to ensure reliable operation of the PPCU as the selected semiconductors (in this case, silicon carbide (SiC) MOSFETs and Si diodes) can only block unidirectional voltages. Out of the eight

International Journal of Engineering Research and Science & Technology

ISSN 2319-5991 www.ijerst.com

Vol. 11, Issue 4, 2018

universal schemes listed in Table I, there are only three feasible schemes that can be used for a dedicated battery charging application. The feasible schemes are depicted in Fig. 3.

Feasibility is dictated by the power flow direction constraint in a PPCU. Solutions that are listed as infeasible in Table I will violate the first constraint as they drain power from the EV battery instead of charging it.

**A)PPCU Performance Metrics**

Let Vout, i and I out, i denote the voltages and currents at the output port of the ith charging unit, Vin, I and Iin,i denote the voltages and currents at the input port of the ith charging unit, Vbat,i and Ibat,i denote the voltages and currents of the ith EV battery as indicated in Fig. 3. The instantaneous power demanded by the ith EV battery, Pbat,i(t) is given by

$$P_{bat,i}(t) = V_{bat,i}(t) I_{bat,i}(t) \quad (1)$$

The instantaneous power at the input and output ports of the charging unit are given by

$$P_{in,i}(t) = V_{in,i}(t) I_{in,i}(t) \quad (2)$$

$$P_{out,i}(t) = V_{out,i}(t) I_{out,i}(t) \quad (3)$$

The expressions for voltages at the input and output ports of the charging unit are given in Table II. Furthermore, the battery current can be expressed in terms of the input and output port currents of the charging unit as follows:

$$I_{bat,i}(t) = \begin{cases} I_{in,i} \text{ (Scheme 1)} \\ I_{in,i} + I_{out,i} \text{ (Scheme 2)} \\ I_{out,i} \text{ (Scheme 3 \& Conventional Scheme)} \end{cases} \quad (4)$$

Let ηi refer to the efficiency of ith charging unit. By invoking power balance relationship (Pout,i = ηiPin,i), the expressions for input and output port currents can be established as in Table II. Let partiality ratio, Ki denote the ratio of power processed by ith charging unit to the power transferred to the ith EV battery

$$K_i = P_{in,i} / P_{bat,i} \quad (5)$$

A lower value of Ki will ensure a very high efficiency for the charger stage. However, practical constraints (such as the permissible swing on the dc bus voltage) exist that may limit the minimum Ki value achievable and is discussed later in Section III. Key converter parameters for assessing the performance of the charging unit are summarized in Table II. In practical PPCUs based on dc–dc converters with galvanic isolation, a non-active power circulation is inevitable at the ac ports in addition to the desired active power flow [14]. The non-active circulating power could degrade the performance of the PPCU in terms of additional losses within the converter.

**B. System Level Benefits**

To showcase the system level benefits with the proposed approach, a case study for a multimegawatt XFC station with six charging points, each rated at 350 kW, is considered. It is assumed that the station is capable of simultaneously charging up

TABLE II

PARAMETERS FOR iTH CHARGING POINT FOR THE PPCU SCHEMES IN Fig. 3

| | $V_{out,i}$ | $V_{in,i}$ | $I_{out,i}$ | $I_{in,i}$ | $K_i$ | Comments |
|---|---|---|---|---|---|---|
| Conventional Scheme | $V_{bat,i}$ | $V_{dc}$ | $I_{bat,i}$ | $\frac{V_{bat,i} I_{bat,i}}{\eta_i V_{dc}}$ | $\frac{1}{\eta_i}$ | Fixed input voltage, variable output voltage |
| PPCU Scheme 1 | $V_{dc}$ | $V_{dc} - V_{bat,i}$ | $\frac{\eta_i I_{bat,i}(V_{dc} - V_{bat,i})}{V_{dc}}$ | $I_{bat,i}$ | $\frac{V_{dc} - V_{bat,i}}{V_{bat,i}}$ | Variable input voltage, fixed output voltage |
| PPCU Scheme 2 | $V_{bat,i}$ | $V_{dc} - V_{bat,i}$ | $\frac{\eta_i I_{bat,i}(V_{dc} - V_{bat,i})}{(1-\eta_i)V_{bat,i} + \eta_i V_{dc}}$ | $\frac{I_{bat,i} V_{bat,i}}{(1-\eta_i)V_{bat,i} + \eta_i V_{dc}}$ | $\frac{V_{dc} - V_{bat,i}}{(1-\eta_i)V_{bat,i} + \eta_i V_{dc}}$ | Variable input voltage, variable output voltage |
| PPCU Scheme 3 | $V_{bat,i} - V_{dc}$ | $V_{dc}$ | $I_{bat,i}$ | $\frac{I_{bat,i}(V_{bat,i} - V_{dc})}{\eta_i V_{dc}}$ | $\frac{V_{bat,i} - V_{dc}}{\eta_i V_{bat,i}}$ | Fixed input voltage, variable output voltage |

TABLE III

SYSTEM LEVEL CASE-STUDY TO SHOWCASE BENEFITS OF PROPOSED PPCU-BASED POWER DELIVERY SCHEME

| Parameter | Conventional Scheme | PPCU Scheme 1 | PPCU Scheme 2 | PPCU Scheme 3 |
|---|---|---|---|---|
| DC Link Voltage, $V_{dc}$ | 800 V | 875 V | 875 V | 650 V |
| Total Charger Peak Power, $\sum_{i=1}^{6} max(P_{in,i})$ | 2.02 MW | 0.36 MW | 0.30 MW | 0.38 MW |
| Cumulative Energy Loss per XFC Cycle, $\sum_{i=1}^{6} E_{loss,i}$ | 13.00 kWh | 1.64 kWh | 1.45 kWh | 2.06 kWh |
| Cumulative Average Power Loss per XFC Cycle, $P_{loss-avg}$ | 78.04 kW | 9.86 kW | 8.71 kW | 12.36 kW |
| Charger Efficiency, $\eta_{charger}$ | 95.0% | 99.3% | 99.4% | 99.2% |

Assumptions: 1) Efficiency, η of each converter (both full power and partial power) is assumed to be 95% at all operating points during one XFC cycle that lasts for 10 minutes.

2) A CC charging pattern with a charging current of 400 A is assumed as shown in Fig. 4(a).

International Journal of Engineering Research and Science & Technology

ISSN 2319-5991 www.ijerst.com

Vol. 11, Issue 4, 2018

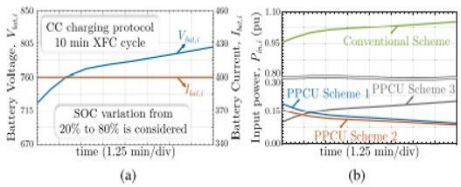


(a) (b)

Fig. 4. (a) 10 min XFC cycle based on CC charging scheme. (b) Power plots of iTH charging unit over an XFC cycle.

To 6 EVs. Currently, there is a trend to move toward 800 V dc system in passenger vehicles to facilitate XFC [21], [22] and hence, such a system is considered for this analysis. Although several techniques have been proposed for the high-power charging mode in XFC systems, a representative, constant-current (CC), 10 min charge cycle presented in Fig. 4(a) is utilized for this article. The minimum battery pack voltage (725 V) corresponds to around 20% state of charge (SoC) while the maximum battery pack voltage (800 V) corresponds to around 80% SoC based on the LNMCO/graphite lithium ion (Li-ion) cell data provided in [23]. In fast charging systems, battery charging is stopped around 80% SoC to eliminate the time consuming, low power, constant-voltage (CV) charging mode. Power processed by a charging unit over one XFC charge cycle for different charging schemes are evaluated based on Table II and plotted in Fig. 4(b). One full XFC charge cycle refers to the worst- case operation where 6 EVs are simultaneously getting charged for a duration of 10 min. typical ratings of a conventional XFC station with six charging points are given in Table III

The total energy transferred to the ith EV battery over one charging cycle, Ebat,i can be expressed as

$$E_{bat,i} = \int_0^{T_{cycle}} P_{bat,i}(t)dt \qquad (6)$$

Where Tcycle is the charging time corresponding to one XFC cycle. The instantaneous power loss in the iTH charging unit can be expressed as

$$P_{loss,i}(t) = (1-\eta_i)P_{in,i}(t) \qquad (7)$$

Since power processed by the partial rated charging unit is much lower than that of the conventional full rated charging unit, the absolute value of the losses is significantly less even with the same charging unit efficiency. The extra energy needed to meet the losses in the iTH charging unit over one full charging cycle can be evaluated as

$$E_{loss,i} = \int_0^{T_{cycle}} P_{loss,i}(t)dt \qquad (8)$$

The cumulative average power loss in all the charging units over one XFC cycle can be computed as

$$P_{loss-avg} = \sum_{i=1}^{6} \frac{E_{loss,i}}{T_{cycle}} \qquad (9)$$

Where Eloss, i is computed based on (8) in kWh. Finally, the efficiency of the charging stage can be computed as

$$\eta_{charger} = \frac{\sum_{i=1}^{6} P_{bat,i}}{\sum_{i=1}^{6} P_{bat,i} + P_{loss-avg}} \qquad (10)$$

Performance parameters are computed for the example system and quantified in Table III. The charger efficiency improves from 95 to > 99% by adopting partial power charging converters.

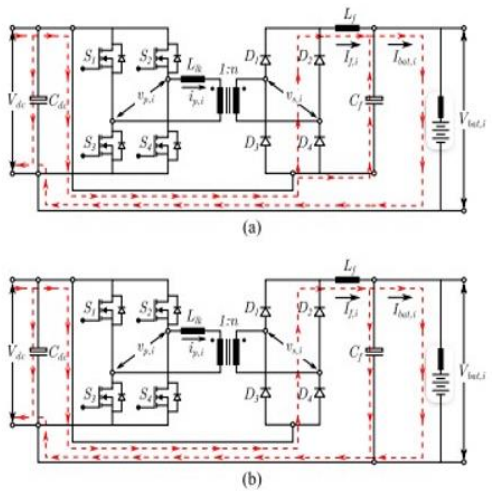

(a) (b)

Fig. 5. Switching ripple propagation path (indicated by red dashed lines) in PPCU. (A) Typical filtering configuration. (B) Proposed filtering configuration.

To 8 fold reduction can be achieved in the average power loss as well as the extra energy that needs to be expended to meet this loss over a charging cycle.

International Journal of Engineering Research and Science & Technology

ISSN 2319-5991 www.ijerst.com

Vol. 11, Issue 4, 2018

The advantages with the proposed scheme are given as follows.

Lower rated charging units can lead to reduced capital costs.

Reduced energy requirements can result in lower operational costs.

Lower power rating of the charger and reduced losses can potentially enable power dense converter solutions as compared to conventional full rated charging units.

**PPCU REALIZATION AND DESIGN CONSIDERATIONS**

A fixed frequency, zero voltage switched, modified PSFB pulse width modulation (PWM) converter topology shown in Fig. 5(b) is chosen as the PPCU candidate. Scheme 3 based terminal connection configuration is chosen as an example. The PSFB-PWM converter is popularly used in high power industrial systems [24] and is a scalable solution to suit XFC application. The primary H-bridge legs of the PSFB-PWM converter are operated with a phase-shift, φ with respect to each other to achieve power transfer. Leg 1 (formed by S1, S3) is termed as the lagging leg and leg 2 (formed by S2, S4) is termed as the leading leg as the pole voltage

(voltage between the output of any leg and the mid potential point of the input dc supply) of leg 2 leads ythat of leg 1. For details on the operation of PSFB-PWM converter, the interested reader is referred to [25]. The design considerations for the PSFB-PWM converter-based PPCU are listed as follows.

Disturbance Propagation and Filtering Arrangement

The typical output filter connection configuration of the PSFB-PWM converter shown in Fig. 5(a) is modified such that the filter capacitor, Cf appears in parallel with the EV battery as in Fig. 5(b). In the typical filtering configuration, there exists a low impedance path for the switching frequency

**TABLE IV**

**DC EV CHARGING STATION BATTERY CURRENT RIPPLE LIMITS**

| Limit, $I_{lim}$ | Frequency |
|---|---|
| 1.5 A | below 10 Hz |
| 6 A | below 5 kHz |
| 9 A | below 150 kHz |

Ripple from the SST stage to directly propagate to the EV battery through the filter capacitor, Cf Furthermore, any disturbance at the input dc link will propagate to the output through this low-impedance path. The proposed filtering configuration offers a true second-order filtering for the switching frequency ripple component.

To showcase the benefits of proposed filtering scheme, a circuit simulation is performed where the PPCU is fed from a dual-active-bridge (DAB) converter-based SST stage. Both the DAB stage and PPCU stage are switched at 50 kHz. The circuit parameters of the PPCU stage for this simulation are provided in Table V. The ripple component in battery current is plotted with the two filter configurations in Fig. 6(a). The presence of a low-impedance path through the output filter accentuates ripple propagation with the typical filter configuration.

Furthermore, in another simulation, the PPCU is fed from an ideal voltage source and a step voltage disturbance is introduced at the input dc link. The circuit parameters for this simulation are provided in Table V. The corresponding battery currents are plotted in Fig. 6(b). Current spikes are observed with the typical filtering configuration as a result of the low impedance path. The proposed filtering scheme attenuates the disturbance as expected.

**Output Filter Design**

The PPCU switching ripple current (peak to peak) in the filter inductor, Lf can be calculated as

$$\Delta I_{f,i} = \frac{\left[nV_{dc} - (V_{bat,i} - V_{dc})\right] D_{eff,i} T_s}{L_f} \qquad (11)$$

Where Vbat, i refers to the voltage of ith battery, Deff, i refers to the effective duty cycle of the ith PPCU as defined in (22), and Ts refers to the switching period of PPCU. The peak-to-peak current ripple limit, Ilim for a dc fast charging

International Journal of Engineering Research and Science & Technology

ISSN 2319-5991 www.ijerst.com

Vol. 11, Issue 4, 2018

station as per IEC 61851-23:2014 is specified in Table IV.

TABLE V: Charging unit circuit parameters.

| Parameter | Partial power charging unit | Full power charging unit |
|---|---|---|
| DC link voltage, $V_{dc}$ | 300 $V$ | 425 $V$ |
| Leakage Inductance, $L_{lk}$ | 3.5 $\mu H$ | 1.7 $\mu H$ |
| Transformer turns ratio, $n$ | 0.35 | 1.0 |
| Filter inductance, $L_f$ | 520 $\mu H$ | 520 $\mu H$ |
| Filter capacitance, $C_f$ | 20 $\mu F$ | 20 $\mu F$ |
| Snubber capacitance, $C_{sn}$ | 47 $nF$ | 47 $nF$ |
| Snubber resistance, $R_{sn}$ | 500 $\Omega$ | 2250 $\Omega$ |
| Switching frequency, $f_{sw}$ | 50 $kHz$ | 50 $kHz$ |
| EV Battery voltage, $V_{bat}$ | $360 - 400$ $V$ | $360 - 400$ $V$ |
| Battery peak power, $P_{bat}$ | 3.2 $kW$ | 3.2 $kW$ |

The output filter should be designed such that ΔIf, i ≤ Ilim based on (11).

Partiality Ratio, Ki

The partiality ratio, Ki of the PSFB-PWM converter shown in Fig. 5(b) decreases with a higher dc bus voltage, which in-turn will improve the system efficiency

$$K_i = \frac{V_{bat,i} - V_{dc}}{\eta_i V_{bat,i}} \qquad (12)$$

However, the selection of an appropriate input dc bus voltage, Vdc is closely linked to the reliable operation of the PPCU. For the chosen PPCU scheme (Scheme 3), the maximum dc bus voltage, Vdc-max is dictated by the minimum battery voltage, Vbat, i−min

$$V_{dc-max} < V_{bat,i-min} \qquad (13)$$

This is to ensure that the voltage at the output dc port (Vout = Vdc − Vbat, i) always remains positive. If the steady-state value of dc bus voltage is chosen very close to Vbat, i−min, there exists a possibility that (13) may be violated under transient conditions or in the presence of any disturbances. Hence, it is recommended that

$$V_{dc} = \frac{V_{bat,i-min}}{(1+x)} \qquad (14)$$

Where x is a safety margin that is chosen based on the maximum permissible voltage swing in the dc bus voltage. This automatically imposes a constraint on the partiality ratio, Ki. The range of Ki as shown in (15) can be obtained by substituting the minimum and maximum values of battery voltage, Vbat,i and the expression for dc bus voltage, Vdc [from (14)] in (12)

In this article, a 20% safety margin (x = 0.2) is assumed.

## III. MODELING AND CONTROL OF PPCU

Individual EV battery current control is achieved by regulating the output filter inductor current of the PFSB-PW converter based PPCU. The small-signal modelling aspects of PSFB-PWM converter have been extensively discussed in the literature .

This effective duty cycle perturbation can now be incorporated within the small-signal model for a PWM buck converter with the proposed terminal connection configuration. An interested reader is directed for the small-signal model derivation for a PWM buck converter. An unterminated, small-signal model for the PSFB-PWM converter that is fed from an ideal voltage source, Vdc is presented in Fig. 7. Small-signal open-loop impedance seen at the output port of ith PPCU can be expressed

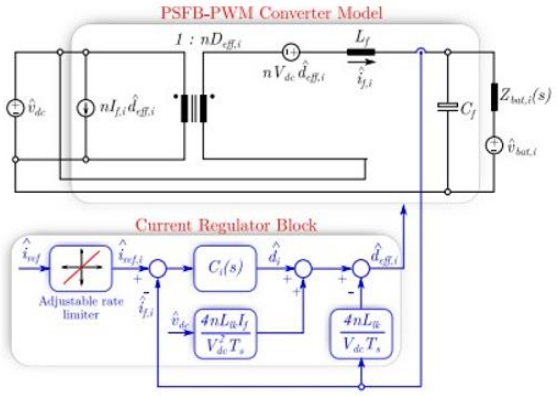


Fig. 6. Unterminated small-signal model of modified PSFB-PWM converter based ith PPCU with output current regulation. Zbat,i(s) refers to battery internal impedance.

The small-signal current-regulator implementation is depicted in Fig. 7.

International Journal of Engineering Research and Science & Technology

ISSN 2319-5991 www.ijerst.com

Vol. 11, Issue 4, 2018

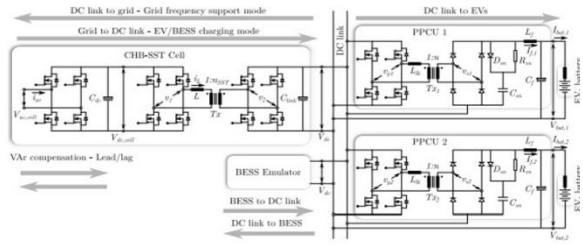


Fig. 7. Laboratory test-bed for the down-scaled XFC station with two charging points. A cell level realization of the ac–dc FEC and dc–dc solid-state transformer is implemented. (a) Circuit topology. (b) CHB-SST cell—hardware prototype. (c) PPCUs—hardware prototype.

## IV.SIMULATION RESULTS

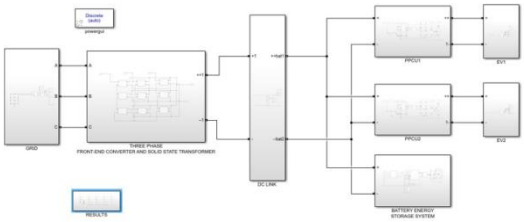

Fig.8 MATLAB/SIMULINK circuit diagram of the proposed system

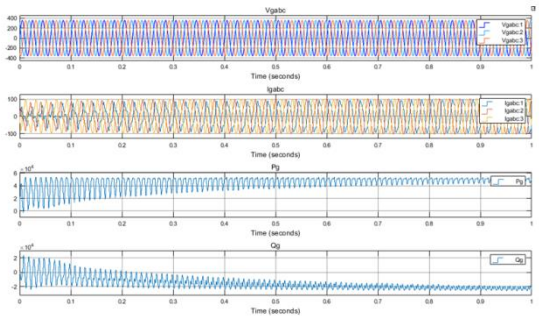


Fig.9 Simulation results of grid

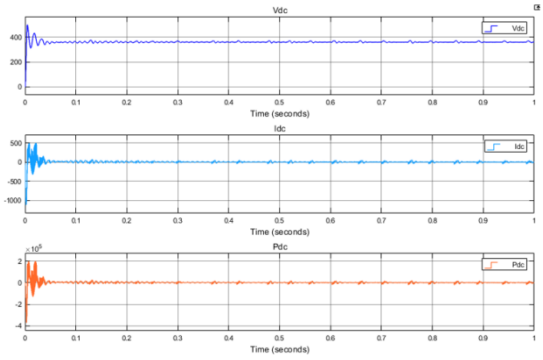


Fig.10 Simulation results of DC link

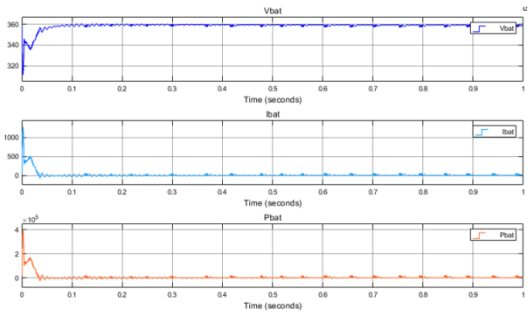


Fig .11 Simulation results of BESS

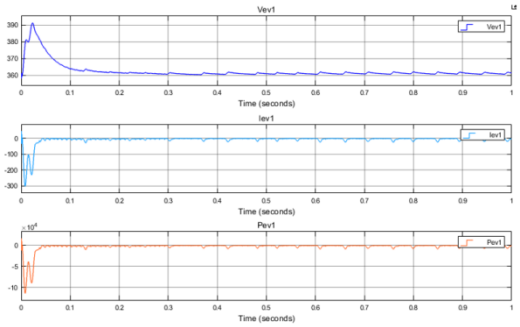


Fig.12 Simulation results of Electric vehicle load-1

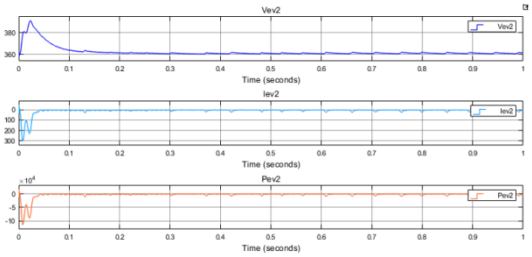


Fig.13 Simulation results of Electric vehicle load-2

## V. CONCLUSION

This article suggested a method for creating a power supply architecture for an XFC station that uses many PPCUs. Utilising the suggested power supply plan will save system costs in terms of construction expenditures, operating expenses, and power and energy efficiency. A viable converter architecture was discovered for the battery charging application, and the characteristics and requirements of employing such a PPCU were examined. The PPCU's design, modelling, and control aspects as they relate to charging the batteries of electric vehicles were examined and debated. Despite its great promise, the XFC power

ISSN 2319-5991 www.ijerst.com

Vol. 11, Issue 4, 2018

delivery system still has to overcome a number of technical and acceptance obstacles before it can be made commercially viable. The suggested partial power charger-based power supply strategy does not provide any galvanic isolation between the different charging ports, even though each charging port is galvanically separated from the grid. According to the IEC 61851-23:2014 standard, requirements for numerous simultaneous outputs that are not separated from one another are being considered for DC charging stations. It is hoped that compelling non-isolated solutions—like the one this article presents—will persuade standards organisations to draft suitable legislation. Furthermore, an 80-kWh Li-ion battery is charged to almost 1.5 C (C stands for charging rate or C-rate) by modern commercial fast charging systems like the 120-kW TESLA supercharger. A battery of this kind would be charged at around 4.4 C by 350-kW XFC units. The battery may degrade more quickly as a consequence of lithium plating, which may occur from charging at such high C-rates. At around 5 C, the battery's efficiency is only 88–93% [31]. In order to allow XFC and ensure the battery operates safely and dependably, this necessitates the combination of next-generation battery management systems with enhanced thermal management technologies. Moving towards XFC stations presents a number of additional difficulties, such as modifying current standards and figuring out a viable business plan. It is necessary to solve issues including communication protocols, safety, standardisation of EV charging equipment, fault management and protection, and interoperability standards.

**REFERENCES**

[1] "Global EV outlook 2017," International Energy Agency, 2017. Accessed: Nov. 27, 2017. [Online].Available:

https://www.iea.org/publications/ free publications/publication/GlobalEVOutlook2017.pdf

[2] L. Dickerman and J. Harrison, "A new car, a new grid," IEEE Power Energy Mag., vol. 8, no. 2, pp. 55–61, Mar./Apr. 2010.

[3] D. Karner, T. Garetson, and J. Francfort, "EV charging infrastructure roadmap," Idaho National Laboratory, 2016. Accessed: Nov. 27, 2017. [Online]. Available: https://avt.inl.gov/sites/default/files/pdf/evse/ EV Charging Infrastructure RoadmapPlanning.pdf

[4] D. Aggeler et al., "Ultra-fast DC-charge infrastructures for EV-mobility and future smart grids," in Proc. IEEE PES Innovative Smart Grid Technol. Conf. Eur., Oct. 2010, pp. 1–8.

[5] M. Vasiladiotis and A. Rufer, "A modular multiport power electronic transformer with integrated split battery energy storage for versatile ultrafast EV charging stations," IEEE Trans. Ind. Electron., vol. 62, no. 5, pp. 3213–3222, May 2015

[6] Evaluating Electric Vehicle Charging Impacts and Customer Charging Behaviours— Experiences from Six Smart Grid Investment Grant Projects, Smart Grid Investment Grant Program, U.S. Department of Energy, Washington, DC, USA, Dec. 2017.

[7] Considerations for Corridor and Community DC Fast Charging Complex System Design, U.S. Department of Energy, Washington, DC, USA, May 2017, pp. 1–51.

[8] S. Bai and S. M. Lukic, "Unified active filter and energy storage system for an MW electric vehicle charging station," IEEE Trans. Power Electron., vol. 28, no. 12, pp. 5793–5803, Dec. 2013.

[9] S. Rivera, B. Wu, S. Kouro, V. Yaramasu, and J. Wang, "Electric vehicle charging station using a neutral point clamped converter with bipolar DC bus," IEEE Trans. Ind. Electron., vol. 62, no. 4, pp. 1999–2009, Apr. 2015.

[10] J. C. G. Justino, T. M. Parreiras, and B. J. C. Filho, "Hundreds kW charging stations for e-buses operating under regular ultra-fast charging," IEEE Trans. Ind. Appl., vol. 52, no. 2, pp. 1766–1774, Mar./Apr. 2016